Materials Science-Poland, 33(3), 2015, pp. 579-587
http://www.materialsscience.pwr.wroc.pl/
DOI: 10.1515/msp-2015-0078

DE GRUYTER OPEN

Effects of partial Co replacement by Fe in $Sr_{0.775}Y_{0.225}CoO_{3-\delta}$ on its magnetic property, oxygen deficiency and crystal structure

I.M. SUTJAHJA*, F. BERTHALITA, M. MUSTAQIMA, A.A. NUGROHO, M.O. TJIA

Physics of Photonics and Magnetism, Dept. of Physics, Faculty of Mathematics and Natural Science, Institute Technology Bandung, Jl. Ganesha 10, Bandung 40132, Indonesia

A study has been conducted on the effects of partial, 10 % Co substitution by Fe in the perovskite $Sr_{0.775}Y_{0.225}CoO_{3-\delta}$ compound. The XRD data show that the resulted samples of Fe-free and Fe-doped compounds exhibit good 314 single phase quality with a tetragonal I4/mmm crystal structure. The measured M-T curves display the typical feature of ferromagnetic (FM) transition at 335 K for the Fe-free sample, while showing significantly degraded FM ordering for the 10 % Fe-doped sample. The oxygen deficiency determined from our 10 % Fe doped sample is found to decrease by only 0.025. Further detailed analysis of the XRD data also reveals distinctly different structural changes in the Co–O slabs compared to the 50 % Fe-doped sample which exhibits a complete suppression of FM order. The results of this study, thus, have revealed the close relations among the changes induced by Fe doping in the magnetic ordering of crystal, and its oxygen content as well as the associated local structure in the Co–O layers responsible for the magnetic properties in the compound.

Keywords: *perovskite $Sr_{0.775}Y_{0.225}CoO_{3-\delta}$ compound; ferromagnetic compound; oxygen content*

1. Introduction

Among many well-known transition metal oxides, perovskite cobalt oxides have emerged as a new distinct class of materials offering a variety of fascinating physical phenomena and potentially useful physical properties, such as ferromagnetism [1], thermoelectricity [2], giant magnetoresistance [3–5] and multiferroism [6]. The rich physical and complex properties of the materials are largely due to the possible presence of multi-valence states of cobalt ions in the compounds, namely Co^{2+}, Co^{3+}, Co^{4+} or the intermediate mixed valence states, which are associated with structural and compositional variations of the system, giving rise to various charge and orbital ordering phases. Besides, this system has the ability to adopt different types of coordination ranging from tetrahedral, pyramidal, to octahedral coordination, making it an attractive candidate for the formation of a number of different structures, with the oxygen nonstoichiometry, playing the role of a crucial parameter for tuning their physical properties. Moreover, various possible states of low-spin (LS, t_{2g}^6), intermediate-spin (IS, $t_{2g}^5e_g^1$), and high-spin (HS, $t_{2g}^4e_g^2$) configurations of cobalt ions may also lead to different electrical transport and magnetic properties, covering ferromagnetic conductor, antiferromagnetism insulator, and multiferroism. These variations of spin states are possible as they are very closely placed in energy and, hence, can be readily changed by temperature, pressure, external magnetic field or oxygen content, resulting in certain modifications of the Co–O atomic distance, O–Co–O bond angle and crystal field splitting. The rich relations among those structural and spin state variations as well as their influences on the compound magnetic properties have been the subjects of intensive research worldwide [7].

Focusing on the magnetic properties, it is worth recalling that the $La_{1-x}Sr_xCoO_3$ system has long been shown to undergo ferromagnetic transition

*E-mail: inge@fi.itb.ac.id

at the highest temperature of $T_C = 250$ K [8]. It has also been more or less established that the ferromagnetic ordering for $x \geqslant 0.18$ is the result of double exchange interaction between the t_g spins of Co^{3+} and Co^{4+} in either their intermediate spin [8, 9] or low spin states [10]. A higher T_C of around 300 K was later reported in cobalt oxide $RBaCo_2O_{5.5}$ (R = rare earth element) [3, 11], where only Co^{3+} was found in the compound, implying the irrelevance of the conventional double exchange interaction for the appearance of ferromagnetic ordering. For R = Tb [5], the ferromagnetic coupling of the spins was suggested to be driven by orbital ordering along the a-axis at 340 K, with antiferromagnetic coupling appearing along the b-axis at 260 K due to superexchange interaction. The bulk ferromagnetic phase is believed to be stabilized at the higher temperature of 300 K as a result of spin state transition of Co^{3+} from IS to HS [5], while LS to HS transition was found in similar range of temperature for R = Gd [3, 11] due to oxygen vacancy ordering reported for this compound [3]. These developments were recently followed by the discovery of new A-site ordered perovskite Co-oxides of $Sr_{1-x}R_xCoO_3$ (R = Y and lanthanide) as independently reported by Withers et al. [12, 13] and Istomin et al. [14, 15]. The evidences and effects of cation ordering in the ab-plane as well as the presence of oxygen vacancies and their ordering were presented in those reports, although the two groups differed in their interpretations of the specific nature of oxygen ordering. It was later shown in a detailed study of $Sr_{2/3}Y_{1/3}CoO_{8/3+\delta}$ compound [16] that a subtle addition of oxygen ($\delta = 0.04$) resulted in the collapse of the orbital ordering found in the compound with $\delta = 0$, and led to an FM-AFM transition along with metal-insulator transition. This system has since attracted a growing interest of researchers owing to the rich structural and magnetic phases as well as the associated charge transport properties [16–18]. An intensified research activity on this system was further stimulated by the observation of room-temperature ferromagnetism in the oxygen deficient $Sr_{1-x}Y_xCoO_{3-\delta}$ compounds (note the different and opposite meaning of δ in this formula compared with that used by Maignan et al. [16]) at 335 K in a very narrow dopant concentration range of $0.2 \leqslant x \leqslant 0.25$ [19]. This is in clear contrast to the case of $La_{1-x}Sr_xCoO_3$, where both its magnetization and associated T_C vary continuously with x over a relatively extended range. This ferromagnetic transition temperature is so far the highest attained among perovskite Co-oxides and promising for future spintronic devices applications [20] and for use as cathode in solid oxide fuel cells [21].

Instead of the double exchange interaction responsible for the ferromagnetism in some perovskite Co oxides ($La_{1-x}Sr_xCoO_3$) [8] as noted earlier, it has been shown that the Co orbital ordering, related to Y/Sr ordering as well as the oxygen deficiency, are most likely to be at the root of the ferromagnetism in the $Sr_{1-x}R_xCoO_3$ (R = Y and lanthanides) system [19, 22, 23]. Recently, detailed analyses based on synchrotron X-ray diffraction [24] and neutron diffraction data [25] have mostly established that the oxygen vacancies are responsible for the creation of a superstructure consisting of oxygen rich octahedral (CoO_6) layers and oxygen deficient tetrahedral ($CoO_{4+\delta}$) layers. The studies further revealed three distinct antiferromagnetic orderings in the tetrahedral layer, which under the influence of the local symmetry give rise to a net ferromagnetic ordering. In an independent study, electrical transport and magnetism of the compound have been shown to be affected by the type and amount of the R dopant [7]. In particular, the doping on the Co sites may have certain effects on the magnetic properties since the partial replacement of Co may either directly weaken the magnetically active constituents in the system, or indirectly induce the unfavorable changes in the oxygen content as well as the structure and orbital orderings in the system. It was reported [26] that 25 % substitution of Co with non-magnetic Ga in the $Sr_{0.75}Y_{0.25}CoO_{2.625+\delta}$ resulted in lowering of ferromagnetic (FM) transition temperature and weakening of the FM ordering, while 50 % replacement of Co by magnetic Fe has instead led to the suppression of the FM order, suggesting important roles of doping induced effects, other than the magnetic properties of the dopant. Indeed, the two

cases were shown to be related to different induced changes in oxygen content and the perovskite structure. Specifically, suppression of FM order shown in the compound with 50 % Co replacement by Fe is accompanied with a large reduction of oxygen deficiency by 0.076, and significant changes in the crystal structure, whereas $\delta \cong 0$ and relatively small changes in the crystal structure were found in the sample of 25 % Co substitution by Ga. Interestingly, more recent studies [27, 28], while confirming the suppression of FM ordering and 0.045 reduction of oxygen deficiency upon 50 % Fe doping of the same compound have also shown that the compound with 12 % Fe doping still exhibits a small residual FM signal somewhat similar to what was found in 25 % Ga doped sample, while undergoing unequally smaller reduction of oxygen deficiency of about 0.020. In view of the scarcity of reports in this doping range, it is desirable to verify or confirm the dopant induced changes particularly at the low level Co replacement by Fe. For that purpose we have conducted a study on the effects of 10 % Fe replacement of the Co ions in $Sr_{0.775}Y_{0.225}CoO_{3-\delta}$, in terms of the induced modification of the magnetic property, in conjunction with changes of the oxygen content and local crystal structure, for comparison with previously reported results cited above.

2. Experimental

The samples of $Sr_{0.775}Y_{0.225}CoO_{3-\delta}$ and $Sr_{0.775}Y_{0.225}(Co_{0.9}Fe_{0.1})O_{3-\delta}$ were synthesized by means of a standard solid-state reaction method. The starting materials were $SrCO_3$, Y_2O_3, Co_3O_4, and Fe_2O_3 powders provided by Sigma Aldrich with purity better than 99.9 %. The two different mixtures were separately prepared according to the corresponding stoichiometric formulae by thorough grinding and mixing before being pelletized for subsequent calcination at 1000 °C for 10 hours. This was followed by sintering process at 1100 °C for 20 hours in air, interrupted by intermediate grindings. The resulted samples were furnace cooled.

The structural characterization of the samples was performed by means of X-ray diffraction (XRD) measurement using Philips machine with CuKα radiation source. The data were taken for diffraction angle (2θ) ranging from 10° to 80°, at a step of 0.02°. Refinement analysis of the XRD patterns was carried out according to Rietveld method [29]. The dc magnetization measurements were performed with a superconducting quantum interference device (SQUID) magnetometer from Quantum Design MPMS. The temperature dependent magnetization (M-T) curves were measured in both zero-field-cooled (ZFC) and field-cooled (FC) modes between 5 and 300 K with an applied H field of 1 kOe. The field dependent magnetization (M-H) curves were measured within H = ±70 kOe at 2 K.

For the determination of oxygen content, the standard iodometric titration method was employed by dissolving about 25 mg of the resulted samples in HCl (1 M) solution containing an excess of KI. This resulted in the reduction of Co^{3+} and Co^{4+} ions in the sample, which were turned into Co^{2+} ions, leading to the formation of a stoichiometric amount of iodine (I_2) in the solution. The iodine was then titrated with $Na_2S_2O_3$ (0.015 M) solution using starch as an indicator which was added just before the end-point.

3. Results and discussion

3.1. XRD characterization

Fig. 1 shows the XRD patterns of Fe-free ($Sr_{0.775}Y_{0.225}CoO_{3-\delta}$) and Fe-doped ($Sr_{0.775}Y_{0.225}Co_{0.9}Fe_{0.1}O_{3-\delta}$) samples. The two samples show closely similar patterns of diffraction peaks and both of them exhibit reasonably good 314 single phase quality, implying a good solid solubility of the 10 % Fe dopant in the samples. The refinement of XRD data for extracting the lattice parameters was carried out by adopting the space group of tetragonal I4/mmm for the crystal structure which had been successfully used in previous works [14].

The specific model employed for the detailed analysis of the XRD data for the Fe-free sample was chosen from among those proposed in the literature [12–14]. It was found that the model best fitted our data was the one proposed by Istomin

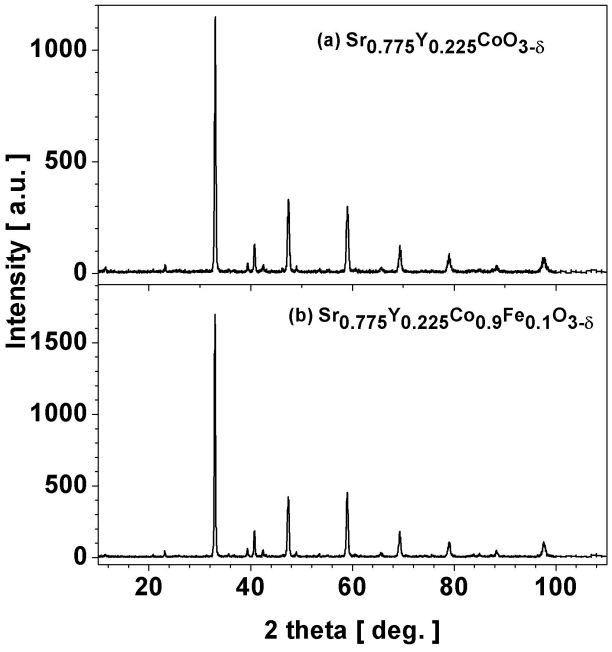

Fig. 1. The XRD patterns of (a) Fe-free ($Sr_{0.775}Y_{0.225}CoO_{3-\delta}$) and (b) Fe-doped ($Sr_{0.775}Y_{0.225}Co_{0.9}Fe_{0.1}O_{3-\delta}$) samples.

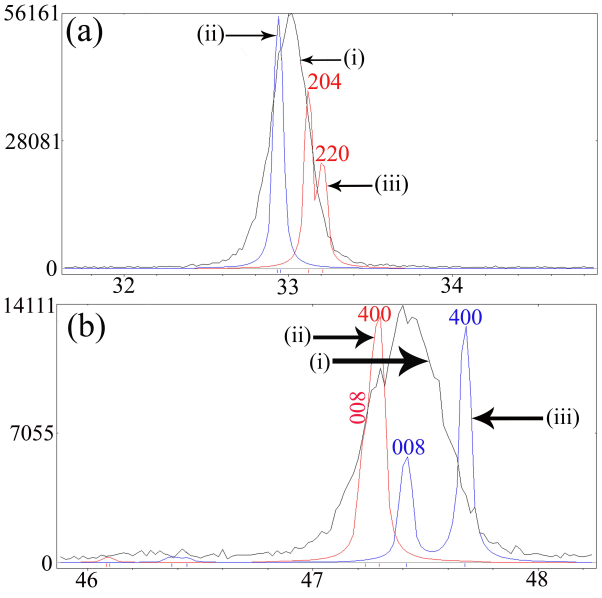

Fig. 2. Comparison of intensity profiles of experimental XRD peaks (i) for Fe doped sample having (a) the highest and (b) the third highest intensity, with those fitted by Lindberg model [26] (ii) and those fitted by the modified Istomin model [14] (iii) as explained in the text.

et al. [14]. For the structural analysis of the Fe-doped sample, on the other hand, comparison was made between the model proposed by Lindberg et al. [26] for $Sr_{0.75}Y_{0.25}Co_{0.5}Fe_{0.5}O_{2.625+\delta}$ sample and that used by Istomin et. al. [14] for $Sr_{0.7}Y_{0.3}CoO_{3-\delta}$ compound with modifications of (Sr,Y) cation distribution, and additional 10 % replacement of Co by Fe as well as small addition of oxygen (O5). These two models were separately applied to fit our data for the Fe doped sample. The resulted fittings of the highest and third highest diffraction peaks are shown in Fig. 2. It is seen that the two XRD intensity profiles are better fitted by the modified Istomin model which has been, henceforth, employed for the ensuing analysis.

The resulted best fitted lattice parameters and the tetragonal distortion as measured by the c/a ratio are summarized in Table 1, together with the associated values of R_p, R_{wp} and χ^2. Further, the observed and calculated XRD patterns using the best fitted parameters as well as their differences are shown in Fig. 3 for both Fe-free and Fe-doped samples. As shown in the figure, the very small intensity differences between the calculated and measured patterns for both samples indicate the quality of the best fitted crystal parameters given in Table 1.

We further note from Table 1 that for $Sr_{0.775}Y_{0.225}CoO_{3-\delta}$ sample, the lattice parameters and tetragonal distortion (c/a) are almost the same with those given in previous report [22] for the same Y dopant concentration which was in the oxygen deficient sample. Upon doping of Fe, the lattice parameter a is seen to decrease slightly, while c increases by even a smaller percentage, resulting in the tiny increase of the tetragonal distortion or c/a ratio. Those changes are likely related to the small differences between the ionic radii of the six-coordinated trivalent Fe^{3+} ions and the Co^{3+} ionic radii in both LS and HS spin states as cited in a previous report [30] (r(Co^{3+} in LS) = 0.545 Å, r(Co^{3+} in HS) = 0.61 Å, r(Fe^{3+} in LS) = 0.55 Å, r(Fe^{3+} in HS) = 0.645 Å). These changes are opposite to those reported by Lindberg et al. [26], but the differences are bordering the limit of our data accuracy and, therefore, are not to be further discussed.

Table 1. Lattice parameters together with the corresponding values of R_p, R_{wp} and χ^2, obtained from refinement of the XRD data of Fe-free ($Sr_{0.775}Y_{0.225}CoO_{3-\delta}$) and Fe-doped ($Sr_{0.775}Y_{0.225}Co_{0.9}Fe_{0.1}O_{3-\delta}$) compounds.

Compounds	$Sr_{0.775}Y_{0.225}CoO_{3-\delta}$	$Sr_{0.775}Y_{0.225}Co_{0.9}Fe_{0.1}O_{3-\delta}$
Lattice parameters (Å)	a = b = 7.655 (4), c = 15.353 (5)	a = b = 7.649 (8), c =15.358 (8)
Tetragonal distortion	c/a = 2.005	c/a = 2.007
χ^2	1.397	1.642
R_p	19.510	20.210
R_{wp}	28.410	28.660

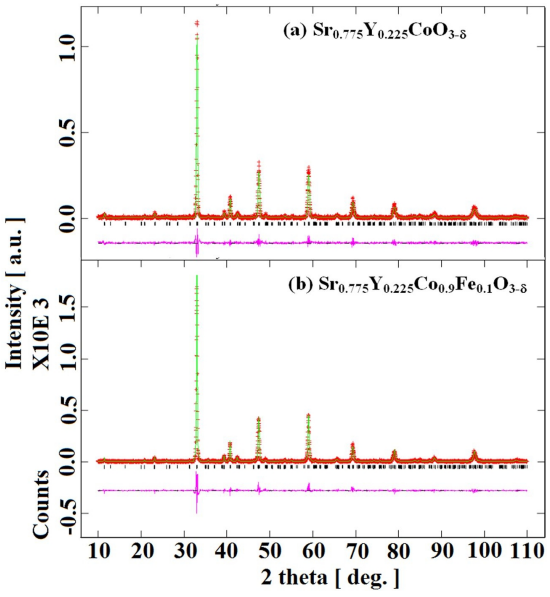

Fig. 3. XRD patterns of Fe-free and Fe-doped samples presented as the observed (crosses) and calculated (full lines) results as well as their differences (bottom trace).

3.2. Magnetization measurement and analysis

The results of magnetization measurements showing the temperature-dependent magnetization (M-T) curves for Fe-free and Fe-doped samples are presented in Fig. 4, and the corresponding field-dependent magnetization (M-H) curves are given in Fig. 5. It is observed from Fig. 4a and Fig. 5a that the $Sr_{0.775}Y_{0.225}CoO_{3-\delta}$ compound exhibits ferromagnetic ordering at the clearly discernable onset temperature of 335 K, in agreement with those reported by Kobayashi et al. [19], Balamurugan [22], and Troyanchuk et al. [27, 28] for the oxygen deficient samples at the same yttrium doping level. Upon 10 % Fe replacement of Co, the measured M-T curve presented in Fig. 4b shows the relatively less rapid rise of the ZFC magnetization around 335 K and its splitting from the FC magnetization curve remains clearly observable at a slightly higher temperature, similar to the result reported for the sample with 12 % Fe-doping [27, 28] and the 25 % Ga replacement of Co [26]. As shown in Fig. 5b, a small but perceptible retention of FM ordering is also observable, although it is marked by a magnetization value about one order of magnitude smaller than that found in $Sr_{0.775}Y_{0.225}CoO_{3-\delta}$. The result presented in Fig. 4b is notably different from the magnetization curves reported for the 50 % Co substitution by Fe, which shows the complete suppression of FM ordering [26, 27]. The cusp-like anomaly occurring at the temperature about 325 K on the ZFC curve is understood to signify the antiferromagnetic contribution [27, 28]. For the two compounds, there is no sign for the existence of spin glass state as found in the $SrCo_{1-x}M_xO_{3-\delta}$ (M = Nb, Ru) system [31], in agreement with the previous report [16]. It seems that with further increase of Fe content, the ferromagnetic ordering becomes smeared out and it turns into a stabilized antiferromagnetic ground state as observed in the 50 % Fe-doped samples reported on the basis of neutron diffraction data [26, 27].

3.3. Modified oxygen deficiency and local structural change

As mentioned earlier on the basis of previously published reports, the appearance of the peculiar

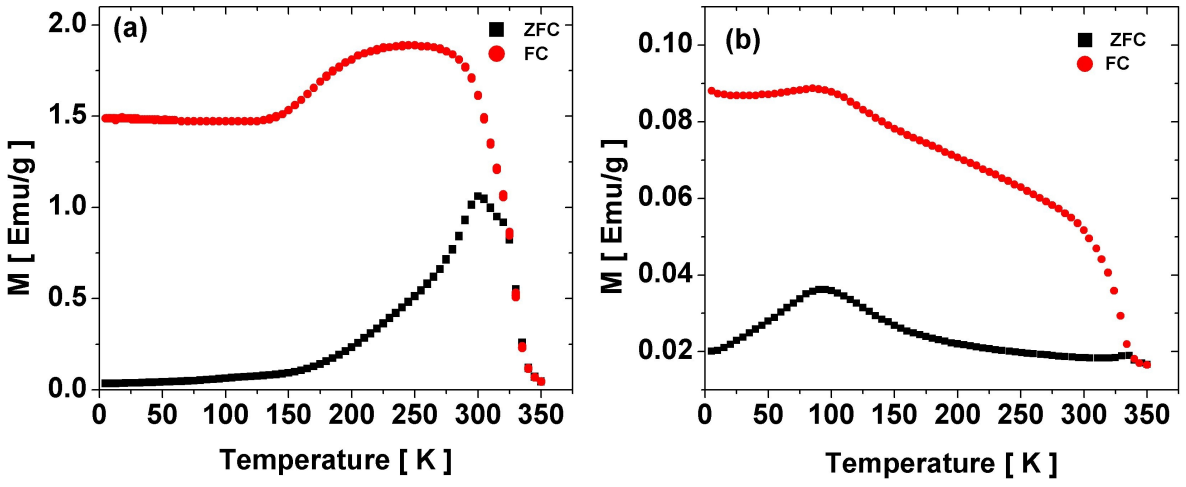

Fig. 4. M-T curves for (a) Fe-free ($Sr_{0.775}Y_{0.225}CoO_{3-\delta}$) and (b) Fe-doped ($Sr_{0.775}Y_{0.225}Co_{0.9}Fe_{0.1}O_{3-\delta}$) samples. The transition of ferromagnetic order for Fe-free sample takes place at $T_C = 335$ K, while the signal is relatively weak in (b).

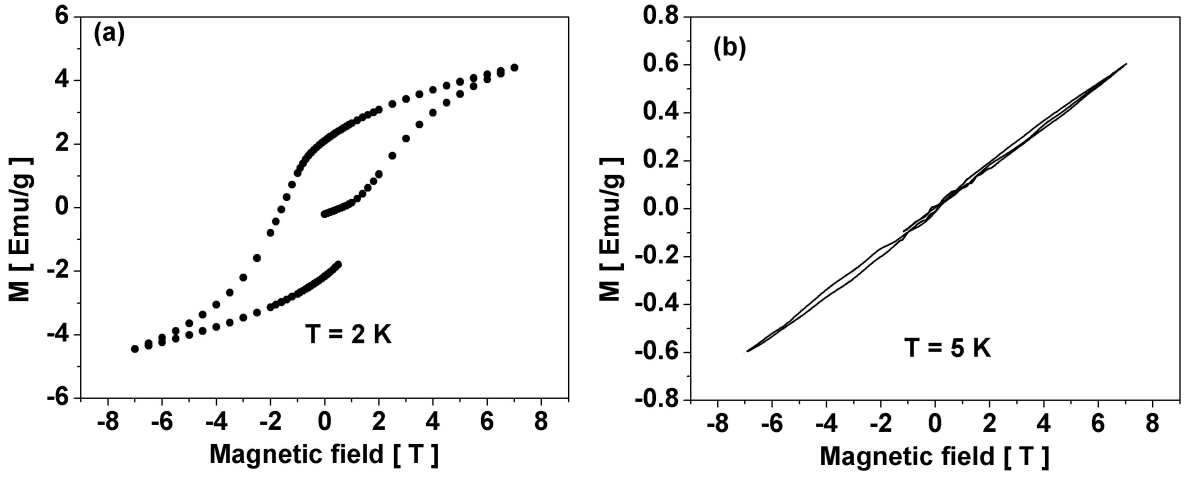

Fig. 5. M-H curves for (a) Fe-free ($Sr_{0.775}Y_{0.225}CoO_{3-\delta}$) and (b) Fe-doped ($Sr_{0.775}Y_{0.225}Co_{0.9}Fe_{0.1}O_{3-\delta}$) samples, each of them measured at temperature of T = 2 K and T = 5 K.

high temperature FM ordering in the 314 cobalt oxide is crucially linked with the specific narrow range of oxygen deficiency, which leads to certain vacancy and cation ordering yielding the net FM ordering in the oxygen deficient $CoO_{4+\delta}$ layer. Given the degree of weakened FM order upon 10 % Fe replacement of Co, it would be worthwhile to find out the corresponding reduction of oxygen deficiency in our sample. This was carried out by the iodometric titration method. For each sample, a series of three titration processes was performed, which showed a reproducibility within an error of about ±0.006 for the oxygen content. The average oxygen-vacancy determined in this experiment gave a δ value of 0.025 for the reduction of oxygen deficiency with respect to that found for the Fe-free sample. This value is considerably less than the values of 0.076 and 0.045 previously reported for 50 % Fe substitution of Co [26–28] and more or less the same with the value of 0.02 for 12 % Fe-doped samples [27, 28], while being slightly larger than the near zero change in Ga-doped sample [26]. All those three samples of low Fe doping and 25 % Ga doping exhibit weak retention of

the ferromagnetic-like contribution in the measured magnetization curves, in a clear contrast to the complete suppression of FM ordering with much larger increase of oxygen content in the 50 % Fe-doped samples [26, 27]. These results, thus, have corroborated the important correlation between the oxygen deficiency and the magnetic property of this compound.

In view of the close connection between the oxygen deficiency and the appearance of structural change, it is tempting at this point to further ascertain the possible signs of the accompanying doping induced structural changes involving the octahedral and tetrahedral layers of Co–O coordination. To this end, the refinement analysis has been conducted at the atomic level on the basis of the same model employed for deducing the result given in Table 1. The resulted atomic positions are given in Table 2 for both Fe free and Fe doped samples, and the associated crystal structures generated using Vesta 3 program [32] are presented in Fig. 6. As shown in the figure, both structures generally consist of alternate stacking of (Sr,Y)O and $CoO_{2-\delta}$ layers. The A-site cations are ordered along the c direction and the ab-plane, which is in good agreement with the results reported previously [12, 14]. Referring to Table 2, Co-ions (Co1 and Co2) in both structures are seen to occupy two different sites in the alternating slabs of octahedral and tetrahedral in agreement with Istomin et al. [14]. These so-called ordered 314 phase structure, associated with the $Sr_{0.75}Y_{0.25}CoO_{3-\delta}$ stoichiometric formula, apparently resembles the Brownmillerite structure found in the mineral $Ca_2[Fe,Al]_2O_5$ which also consists of alternating layers of tetrahedral and octahedral. In the 314 structure, however, the Co ions in the tetrahedral section form the tetracyclic Co_4O_{12} units due to Sr^{2+} and Y^{3+} ordering, instead of the formation of infinite Co chains in the tetrahedral section found in the brownmillerite structure [14, 33].

A further analysis of the interatomic distances between the Co cation and the neighboring anions as well as the bond angles at the Co cation vertices indicates perceptible differences in the changes of Co–O_2 bond lengths similar to changes previously

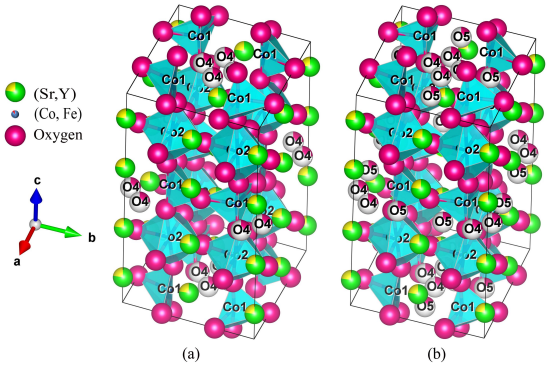

Fig. 6. Crystal structures of (a) $Sr_{0.775}Y_{0.225}CoO_{3-\delta}$ and (b) $Sr_{0.775}Y_{0.225}Co_{0.9}Fe_{0.1}O_{3-\delta}$ constructed on the basis of parameters presented in Table 2.

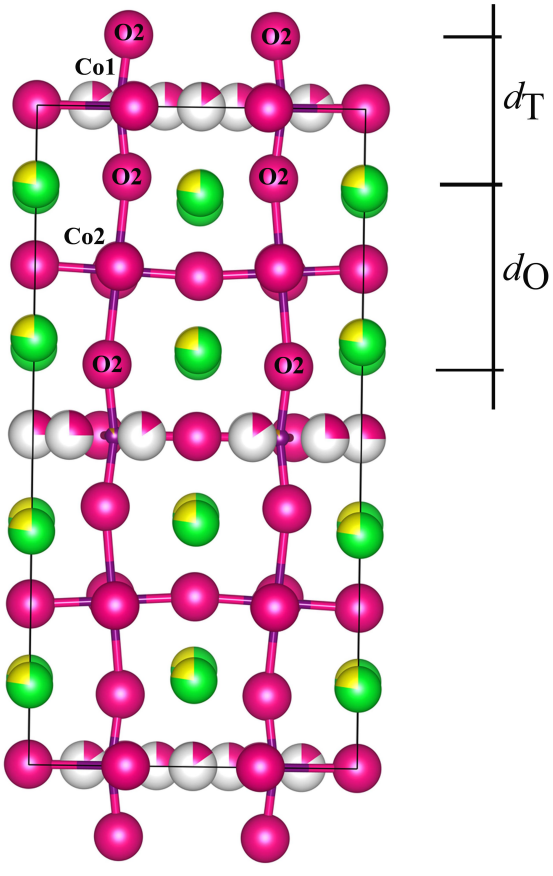

Fig. 7. Front side of the crystal structure of the ordered 314 phase. The symbols d_O and d_T denote the thicknesses of the slabs of octahedral and tetrahedral, respectively.

Table 2. Atomic positions and coordinates of Fe-free and Fe-doped compounds.

Atomic positions		$Sr_{0.775}Y_{0.225}CoO_{3-\delta}$	$Sr_{0.775}Y_{0.225}Co_{0.9}Fe_{0.1}O_{3-\delta}$
Sr1/Y1, 4e; 0, 0, z		0.880 (10)	0.879 (4)
Sr2/Y2, 8g; 0, 0.5, z		0.866 (7)	0.869 (3)
Sr3/Y3, 4e; 0, 0, z		0.356 (3)	0.353 (9)
Co1(/Fe1), 8h; x, x, 0		0.748 (11)	0.748 (3)
Co2(/Fe2), 8f; 0.25, 0.25, 0,25			
O1, 16n; 0, y, z	y	0.245 (6)	0.257 (4)
	z	0.244 (4)	0.107 (9)
O2, 16m; x, x,	x	0.272 (7)	0.277 (7)
	z	0.110 (5)	0.107 (8)
O3, 8i; 0, y, 0	y	0.700 (7)	0.705 (5)
O4, 8j; x, 0.5, 0	x	0.385 (15)	0.390 (14)
		(Occupancy factor: 0.25)	(Occupancy factor: 0.25)
O5, 8j; x, 0.5, 0	x		0.169 (30)
			(Occupancy factor: 0.151*)

*The value was taken from Lindberg et al. [26].

reported for 12 % Fe-doped and 25 % Ga-doped samples but different from those reported for 50 % Fe-doped samples. The consequence of this difference results in perceptible structural changes of octahedral (d_O) and tetrahedral (d_T) slabs, as depicted in Fig. 7. Specifically, the slab thickness calculated as the distance between the O2 ions in each slab gives the estimated values of $d_O = 4.31$ Å, $d_T = 3.39$ Å for the Fe-free sample, and $d_O = 4.41$ Å, $d_T = 3.31$ Å for the Fe-doped sample. We note that the same trend, marked by an increase of octahedral block layer and the decrease of tetrahedral block layer is also found in the 25 % Ga-doped compound, while both slabs were found to be elongated in the sample with 50 % Co replacement by Fe [26].

It is worth noting in this connection that recent reports [25, 27, 28] have shown that the Co ions in the octahedral slab are non-magnetic as they are in the LS state, while Co ions in the tetrahedral slab are magnetic. Related to those structural changes, the magnetic effect of the dilation of octahedral block may be slightly compensated by that of the shrinkage of the tetrahedral block, which results in smaller net increase in the distance between the magnetic Co ions compared to what happens in the 50 % Fe-doped sample. This may roughly explain the observed residual ferromagnetic ordering in this sample instead of the complete suppression of FM ordering in the 50 % Fe-doped sample.

4. Conclusion

We have presented the measurement results of effects induced by 10 % Fe substitution of Co in a perovskite $Sr_{0.775}Y_{0.225}CoO_{3-\delta}$ compound. The M-T and M-H data of the sample exhibit tiny hysteretic behavior, with the magnetization value reduced by one to two orders of magnitude in comparison to those measured for the Fe-free sample, similar to the results for 12 % Fe doped sample and 25 % Ga doped sample reported previously. This is in a clear contrast to the case of complete suppression of FM order reported for 50 % Fe-doped sample. It has been shown that relatively small reduction of oxygen deficiency of 0.025 is found in our sample, similar to that reported for 12 % Fe doped sample, but substantially smaller than the value of 0.045 to 0.076 reported for 50 % Fe doped samples. Further, the structural analysis performed on the basis of XRD data also indicates perceptible changes in the octahedral and tetrahedral

Co–O slabs which are different from those found for the 50 % Fe doped compound, and may offer some hints regarding different effects on the FM orderings in those different compounds.

Acknowledgements

We thanks to Dr. H. Setianto (Dept. of Chemistry, ITB) and Dr. S. Wonorahardjo (Dept. of Chemistry, State Univ. of Malang) for the iodometric titration experiment (HS) and its analysis (SW). The results in this research are funded by the Science and Technology Research Grant from Indonesia Toray Science Foundation (ITSF) 2013 and Riset dan Inovasi KK ITB 2013 Research Program under Contract Number: 229/I.1.C01/PL/2013.

References

[1] KRIENER M., ZOBEL C., REICHL A., BAIER J., CWIK M., BERGGOLD K., KIERSPEL H., ZABARA O., FREIMUTH A., LORENZ T., *Phys. Rev. B*, 69 (2004), 094417.

[2] ANDROULAKIS J., MIGIAKIS P., GIAPINTZAKIS J., *Appl. Phys. Lett.*, 84 (2004), 1099.

[3] TASKIN A.A., LAVROV A.N., ANDO Y., *Phys. Rev. Lett.*, 90 (2003), 227201.

[4] TROYANCHUK I.O., KASPER N.V., KHALYAVIN D.D., SZYMCZAK H., SZYMCZAK R., BARAN M., *Phys. Rev. Lett.*, 80 (1998), 3380.

[5] MORITOMO Y., AKIMOTO T., TAKEO M., MACHIDA A., NISHIBORI E., TAKATA M., SAKATA M., OHOYAMA K., NAKAMURA A., *Phys. Rev. B*, 61 (2000), R13325.

[6] CAIGNAERT V., MAIGNAN A., SINGH K., SIMON C., PRALONG V., RAVEAU B., MITCHELL J.F., ZHENG H., HUQ A., CHAPON L.C., *Phys. Rev. B*, 88 (2013), 174403.

[7] RAVEAU B., SEIKH M., *Cobalt Oxides: From Crystal Chemistry to Physics*, Wiley-VCH Verlag & Co., Weinheim, 2012.

[8] WU J., LEIGHTON C., *Phys. Rev. B*, 67 (2003), 174408.

[9] ITOH M., NATORI I., KUBOTA S., MOTOYA K., *J. Phys. Soc. Jpn.*, 63 (1994), 1486.

[10] SEÑAŔIS-RODŔIGUEZ M.A., GOODENOUGH J.B., *J. Solid State Chem.*, 118 (1995), 323.

[11] FRONTERA C., GARCÍA-MUŃOZ J.L., LLOBET A., ARANDA M.A.G., *Phys. Rev. B*, 65 (2002), 180405(R).

[12] WITHERS R.L., JAMES M., GOOSENS D.J., *J. Solid State Chem.*, 174 (2003), 198.

[13] JAMES M., CASSIDY D., GOOSENS D.J., WITHERS R.L., *J. Solid State Chem.*, 177 (2004), 1886.

[14] ISTOMIN S.Y., GRINS J., SVENSSON G., DROZHZHIN O.A., KOZHEVNIKOV V.L., ANTIPOV E.V., ATTFIELD J.P., *Chem. Mater.*, 15 (2003), 4012.

[15] ISTOMIN S.Y., DROZHZHIN O.A., SVENSSON G., ANTIPOV E.V., *Solid State Sci.*, 6 (2004), 539.

[16] MAIGNAN A., HÉBERT S., CAIGNAERT V., PRALONG V., PELLOQUIN D., *J. Solid State Chem.*, 178 (2005), 868.

[17] GOOSSENS D.J., WILSON K.F., JAMES M., STUDER A.J., WANG X.L., *Phys. Rev. B*, 69 (2004), 134411(1-6).

[18] ZHANG Y., SASAKI S., ODAGIRI T., IZUMI M., *Phys. Rev. B*, 74 (2006), 214429.

[19] KOBAYASHI W., ISHIWATA S., TERASAKI I., TAKANO M., GRIGORAVICIUTE I., YAMAUCHI H., KARPPINEN M., *Phys. Rev. B*, 72 (2005), 104408.

[20] ŽUTIĆ I., FABIAN J., SARMA DAS S., *Rev. Mod. Phys.*, 76 (2004), 323.

[21] STAMBOULI A.B., TRAVERSA E., *Renew. Sust. Energ. Rev.*, 6 (2002), 433.

[22] BALAMURUGAN S., *World J. Condens. Mat. Phys.*, 1 (2011), 145.

[23] KOBAYASHI W., YOSHIDA S., TERASAKI I., *J. Phys. Soc. Jpn.*, 75 (2006), 103702.

[24] ISHIWATA S., KOBAYASHI W., TERASAKI I., KATO K., TAKATA M., *Phys. Rev. B*, 75 (2007), 220406(R).

[25] KHALYAVIN D.D., CHAPON L.C., SUARD E., PARKER J.E., THOMPSON S.P., YAREMCHENKO A.A., KHARTON V.V., *Phys. Rev. B*, 83 (2011), 140403(R).

[26] LINDBERG F., DROZHZHIN O.A., ISTOMIN S.YA., SVENSSON G., KAYNAK F.B., SVEDLINDH P., WARNICKE P., WANNBERG A., MELLERGÅRD A., ANTIPOV E.V., *J. Solid State Chem.*, 179 (2006), 1434.

[27] TROYANCHUK I.O., KARPINSKY D.V., DOBRYANSKIĬ V.M., CHOBOT A.N., CHOBOT G.M., SAZONOV A.P., *J. Exp. Theor. Phys+*, 108 (2009), 428.

[28] TROYANCHUK I.O., KARPINSKY D.V., SAZONOV A.P., SIKOLENKO V., EFIMOV V., SENYSHYN A., *J. Mater Sci.*, 44 (2009), 5900.

[29] LARSON A.C., DREELE VON R.B., *General Structure Analysis System (GSAS)*, Los Alamos National Laboratory Report, LAUR 86-748, 1994.

[30] SHANNON R.D., *Acta Crystallogr. A*, 32 (1976), 751.

[31] MOTOHASHI T., CAIGNAERT V., PRALONG V., HERVIEU M., MAIGNAN A., RAVEAU B., *Phys. Rev. B*, 71 (2005), 214424.

[32] MOMMA K., IZUMI F., *J. Appl. Crystallogr.*, 44 (2011), 1272.

[33] FUKUSHIMA S., SATO T., AKAHOSHI D., KUWAHARA H., *J. Appl. Phys.*, 103 (2008), 07F705(1-3).

Received 2014-11-25
Accepted 2015-05-05